A ROLE FOR ARTEMIS IN REPAIR OF DNA DOUBLE-STRAND BREAKS BEARING 3′-PHOSPHOGLYCOLATE TERMINI*

Lawrence F. Povirk[2], Tong Zhou[2], Ruizhe Zhou[2], Morton J. Cowan[3] and Steven M. Yannone[1*]

From the [1]Life Sciences Division, Lawrence Berkeley National Laboratory, Berkeley CA 94720 and the [2]Department of Pharmacology and Toxicology, Massey Cancer Center, Virginia Commonwealth University, Richmond, VA 23298 and the Department of Pediatrics, University of California San Francisco, San Francisco, CA 94143

Running title: Artemis Processing of 3′-Phosphoglycolate Termini

*Address correspondence to: Steven M. Yannone, Life Sciences Division, Department of Molecular Biology, Lawrence Berkeley National Laboratory, Mail stop 74-157, 1 Cyclotron Road, Berkeley, California 94720, Tel: (510) 495-2867, Fax: (510) 486-6816, E-mail: SMYannone@lbl.gov

The Artemis nuclease is required for V(D)J recombination and for repair of an as yet undefined subset of radiation-induced DNA double-strand breaks. To assess the possibility that Artemis functions on oxidatively modified double-strand break termini, its activity toward model DNA substrates, bearing either 3′-hydroxyl or 3′-phosphoglycolate moieties, was examined. A 3′-phosphoglycolate had little effect on Artemis-mediated trimming of long 3′ overhangs (>9 nucleotides), which were efficiently trimmed to 4-5 nucleotides. However, 3′-phosphoglycolates on overhangs of 4-5 bases promoted selective Artemis-mediated trimming of a single 3′-terminal nucleotide, while at least 2 nucleotides were trimmed from identical hydroxyl-terminated substrates. Artemis also efficiently removed a single nucleotide from a phosphoglycolate-terminated 3-base 3′ overhang, while leaving an analogous hydroxyl-terminated overhang largely intact. Such removal was dependent upon Ku, DNA-dependent protein kinase, and ATP. Together, these data suggest that Artemis-mediated cleavage of 3′ overhangs requires a minimum of 2 nucleotides, or a nucleotide plus a phosphoglycolate, 3′ to the cleavage site. Shorter 3′-phosphoglycolate-terminated overhangs and blunt ends were also processed by Artemis, but much less efficiently. Consistent with the in vitro substrate specificity of Artemis, human cells lacking Artemis exhibited hypersensitivity to X-rays, bleomycin and neocarzinostatin, which all induce 3′-phosphoglycolate-terminated double-strand breaks. Collectively, these results suggest that 3′-phosphoglycolate termini and/or specific classes of DNA ends that arise from such blocked termini are relevant Artemis substrates in vivo.

The Artemis genetic locus was identified by virtue of its association with a form of B− T− NK+ severe combined immune deficiency (SCID) in humans, designated RS-SCID (radiation-sensitive SCID) (1) or SCIDA (Athabascan SCID) (2). The Artemis protein is a nuclease that is activated by DNA-dependent protein kinase (DNA-PK) and is required for the opening of hairpin ends formed during V(D)J recombination (3), thus accounting for the SCID phenotype associated with Artemis deficiency. SCIDA and RS-SCID fibroblasts are radiation-sensitive, but fail to repair only a small fraction of radiation-induced DNA double-strand breaks (DSBs) (4-6). In vitro, activated Artemis removes 5′ overhangs from DNA ends and shortens 3′ overhangs (3), raising the possibility that during DSB repair in vivo, Artemis may trim overhangs that otherwise cannot be processed to give ligatable ends.

About half of DNA breaks induced by ionizing radiation bear 3′-phosphoglycolate (3′-PG) termini (7) that must be removed in order to allow gap-filling by DNA polymerases μ and λ, and ligation by DNA ligase IV (8). While tyrosyl-DNA phosphodiesterase (TDP1) is the only identified enzyme capable of processing 3′-PGs on 3′ overhangs (9), TDP1-mutant cells show only marginal radiosensitivity (10), suggesting the existence of an alternative pathway for processing of these lesions in vivo.

Because Artemis-deficient cells exhibit significant sensitivity to ionizing radiation, yet have only a small DSB repair defect, we assessed the possibility that Artemis functions in processing overhanging 3′-PG termini. We purified recombinant Artemis and examined the activity of

this protein on a variety of oligomeric and plasmid substrates bearing 3′-overhangs. We further investigated the relevance of Artemis to the repair of 3′-PG terminated DSBs by measuring the toxicity of drugs known to induce such breaks in normal and Artemis-deficient cells.

EXPERIMENTAL PROCEDURES

Protein expression and purification—Artemis expression constructs were derived from full-length Artemis cDNA as described previously (2). Full-length Artemis protein was purified from SF9 insect cells infected with recombinant baculovirus generated by sub-cloning Artemis cDNA into pFASTBAC-HT (GIBCO-BRL). Briefly, the amino-poly-histidine tagged Artemis was extracted and purified using IMAC chromatography with standard protocols (Ni-NTA, Pharmacia). Fractions containing Artemis were dialyzed into 50 mM HEPES, pH 7.5, 10% glycerol, 2 mM EDTA, 1 mM dithiothreitol, 0.01% Nonidet P-40, 20 μg/ml phenylmethylsulfonyl fluoride, 1 μg/ml aprotinin, pepstatin A, and leupeptin (HCB), containing 0.1 M NaCl. The affinity-purified protein was loaded onto a Mono Q column (Pharmacia) and eluted with a linear gradient of 100-500 mM NaCl in HCB. Aliquots of Artemis-containing fractions were snap frozen and stored at −70°C. Ku 70/80 was purified from insect cells co-infected with a mixture of recombinant baculovirus harboring the human Ku70 and Ku80 genes and DNA-PKcs was purified from HeLa cells, both as described previously (11). XRCC4 / DNA ligase IV complex was also expressed from baculovirus and purified as described (12). All proteins were assayed for activity and concentration, aliquotted, snap frozen and stored at –70°C.

DNA substrates—Oligonucleotides were purchased from Qiagen or Integrated DNA technologies. All labeled oligomers were purified by gel electrophoresis followed by reverse-phase HPLC. To generate 3′-PG oligomers with the sequence CGAGGAACGCG(A_n)CG ($0 \le n \le 4$), 5′-^{32}P-end-labeled oligomers CGAGGAACGCG(A_n)CGCCC were treated with bleomycin plus H_2O_2, and the desired 3′-PG products were isolated from a sequencing gel and purified by HPLC (13). An analogous oligomer (n=1) bearing a 3′-phosphotyrosine terminus was purchased from Midland Certified Reagents. The 36-base 3′-PG or 3′-hydroxyl oligomers were prepared by ligating the corresponding labeled 14-mers to the 22-mer GCCATGTACTTGGATGA-TCTAT in the presence of the complementary 20-mer GCGTTCCTCGATAGATCATC, and were again gel/HPLC-purified. Partial duplexes were annealed in 10 mM Tris-HCl pH 8, 0.1 M NaCl, 1 mM EDTA by heating to 80°C followed by slow cooling to 10°C over a period of 3 hr. Internally labeled plasmid substrates with various overhangs were constructed by ligating 3′-PG, 3′-phosphotyrosyl or 3′-hydroxyl oligomers (9-24 bases in length) into plasmids with an 11-base 5′ overhang, as described (14).

Nuclease assays—Reaction mixtures (10 μl) containing 25 mM Tris-HCl pH 8, 25 mM NaCl, 10 mM $MgCl_2$, 1 mM dithiothreitol, 0.25 mM ATP, 50 μg/ml BSA and either 5 nM oligomeric substrate or 1 nM plasmid substrate were prepared at 22°C. In some cases, a blunt-ended double-stranded 35-mer (4 nM - 1 μM) was also included (3). Ku (13 or 65 nM) was added and the mixture was immediately vortexed and briefly centrifuged. DNA-PKcs (35 or 50 nM) was then added followed immediately by Artemis (90 or 240 nM), and the reaction was mixed by pipetting and placed in a 37°C bath. Reactions with oligomeric substrates were stopped by addition of 10 μl formamide containing 20 mM EDTA, and the DNA was heat-denatured and analyzed on sequencing gels. Reactions containing plasmid substrates were stopped by addition of 20 μl of 10 mM EDTA, 0.45 M sodium acetate, 100 μg/ml tRNA, followed immediately by phenol extraction and ethanol precipitation. DNA was cut with AvaI (20 units, 6 hr, 37°C) or Taq$^{\alpha}$I (20 units, 4 hr, 65°C) in 50 μl of the buffer supplied by the vendor (New England Biolabs). In some cases 0.25 mM $CoCl_2$ and 0.1 mM ddGTP were subsequently added and the samples were treated with 20 units terminal deoxynucleotidyl transferase (New England Biolabs) for 1 hr at 37°C. DNA was precipitated, dissolved in formamide, heat-denatured and analyzed on sequencing gels. The AvaI and Taq$^{\alpha}$I cleavage sites differ by one nucleotide; however, as expected these two enzymes always gave essentially identical results in parallel experiments.

End joining in cell extracts—Internally labeled plasmid substrates, bearing either PG- or hydroxyl-terminated 3-base 3′ overhangs on both ends, were constructed (14). The substrate (10 ng) was incubated for 6 hr at 37°C in HeLa nuclear

extracts (Promega; final protein concentration 1.4 mg/ml) supplemented with dNTPs and 25 nM (5 μg/ml) recombinant XRCC4 / ligase IV complex (15), which is required for efficient end joining in these extracts (16). Substrates were deproteinized, cut with BstXI and Taq$^{\alpha}$I, and analyzed on a sequencing gel.

Cell Lines and proliferation assays—Fibroblast lines were established from skin biopsies from SCIDA patients 04 and 05 and an unrelated immunologically normal individual (AK). Early passage cultures were immortalized by introduction of hTERT cDNA using methods previously described (6, 11). Cells were either irradiated using a Pantak® X-ray generator operating at 320 kV/10 mA with 0.5 mm copper filtration or exposed to genotoxic drugs for one hour, washed 3 times with PBS, then labeled by the addition of fresh medium containing 10 μg/ml bromodeoxyuridine (BrdU) (Sigma) for 35-45 hours. Cells were harvested, fixed, and stained using standard procedures and cell cycle distribution and BrdU incorporation were analyzed with a Beckman-Coulter EPICS XL-MCL flow cytometer using XL Data Acquisition software and WinMDI 2.8 software. The fraction of proliferating cells was calculated by scoring the percent of intact cells staining positive for BrdU and normalizing to the untreated control of the same cell line (≥ 10,000 events were scored for each point).

RESULTS

Ku-dependent trimming of 3′-hydroxyl-terminated overhangs by purified recombinant Artemis—To assess the specificity of recombinant Artemis, partial duplexes with 3′-hydroxyl-terminated 3′ overhangs of 13, 15 and 17 bases were prepared and treated with Artemis in the presence of Ku, DNA-PKcs and ATP (Fig. 1A). In initial experiments, an excess of a 35-bp duplex was included to ensure robust activation of DNA-PK and subsequent phosphorylation of Artemis (3). Reactions containing Ku, DNA-PKcs, substrate, and 35-bp duplex showed no detectable nuclease activity (Fig. 1A and B). Addition of purified recombinant Artemis resulted in a small but detectable fraction of a 13-base 3′ overhang being shortened to a 5-, 6- or 7-base overhang (28-, 29- and 30-mer fragments; Fig. 1A). A 15-base 3′ overhang was similarly shortened, predominantly to a 5-base overhang (26-mer). Notably, the extent of cleavage increased over time, but there was little change in the cleavage pattern, suggesting that endo- rather than exonucleolytic cleavage predominated. There was very little processing of a substrate with a 17-base 3′ overhang, suggesting that the 19-bp duplex portion of this substrate may have been too short to accommodate the full Artemis-DNA-PK complex.

Previous work with immunoconjugated Artemis bound to agarose beads indicated similar shortening of a long 3′ overhang, in a reaction that required ATP and catalytically active DNA-PKcs, but was independent of the presence or absence of Ku (3). However, in reactions with soluble histidine-tagged recombinant Artemis, the presence of Ku dramatically stimulated Artemis endonuclease activity, but only when the blunt-ended 35-bp duplex was absent (Fig. 1B). Rather than being required for DNA-PK activation, an excess of 35-bp duplex DNA inhibited Artemis nuclease activity in reactions containing Ku, but did not perturb the much weaker Artemis nuclease activity seen in the absence of Ku (Fig. 1B). The potent concentration-dependent inhibitory effect of the duplex in the presence of Ku (Fig. 1C) suggests that the endonucleolytically active Ku/DNA-PKcs/Artemis complex has a high affinity for DNA ends and is effectively competed away from the labeled DNA substrate by an excess of the 35-bp duplex. The residual activity seen in the absence of Ku may be catalyzed by a species (either Artemis/DNA-PKcs or free activated Artemis) that has a much lower affinity for DNA ends, or preferential specificity for 3′ overhangs, and is thus less subject to inhibition by a competing blunt-ended substrate. In any case, the 3′-overhang substrates, at a concentration of 5 nM, were apparently sufficient for robust DNA-PK and Artemis activation. Thus, in most subsequent experiments, the 35-bp duplex was omitted.

Trimming of long 3′-PG-terminated overhangs—DSBs induced by radiation and other free radical-based toxins commonly bear 3′-PG termini (7,17-19) which block polymerase and ligase activities as well as most human exonucleases. To determine whether the endonucleolytic activity of Artemis was affected by the presence of PG termini, similar partial duplexes bearing 3′ overhangs with 3′-PG termini were constructed, by ligating a 5′-end-labeled 3′-PG 14-mer to an unmodified 22-mer. The resulting internally labeled 36-mer was annealed

to 21-, 23- and 27-base complementary strands to yield substrates with PG-terminated 15-, 13- and 9-base 3′ overhangs. A parallel set of substrates with 3′-hydroxyl termini were also constructed, differing from the 3′-PG substrates only in the chemistry of the termini.

As expected, Artemis treatment of these 3′-hydroxyl substrates resulted in efficient trimming of overhangs (Fig. 2A). The 15-base (36/21 substrate) and 13-base (36/23 substrate) overhangs were each predominantly shortened to a 5-base overhang (26- and 28-base products, respectively). The similarity of the cleavage pattern to that seen with the 5′-end-labeled substrates (Fig. 1B) suggests that there was little if any 5′→3′ degradation of the labeled strand. The 9-base overhang (36/27p substrate) was trimmed predominantly to a 4-base overhang (31-mer) rather than 5-base overhang.

Overhangs bearing 3′-PG termini were also trimmed by Artemis (Fig. 2B). The 15- and 13-base overhangs were each trimmed predominantly to 5-base overhangs, while the 9-base overhang was trimmed to a 4-base overhang. These cleavage patterns are essentially identical to those obtained with the analogous 3′-hydroxyl overhangs, indicating that the PG terminus had little effect on the efficiency and specificity of Artemis-mediated DNA cleavage of long 3′ overhangs.

Single-nucleotide trimming of short 3′-PG-terminated 3′ overhangs—To assess Artemis-mediated processing of shorter overhangs, an internally labeled plasmid with a 3-base PG-terminated 3′ overhang, previously used for in vitro studies of nonhomologous end joining (20), was employed (Fig. 3). In addition to more closely mimicking the DSB ends that would be encountered by Artemis in vivo, the plasmid substrate eliminates the possibility of interference between DNA-PK complexes loading from opposite ends of the DNA molecule, which could occur with the oligomeric substrates. This substrate was treated with Artemis and DNA-PK, phenol-extracted, and cut with AvaI or Taq$^{\alpha}$I. The 15-base (AvaI) or 14-base (Taq$^{\alpha}$I) fragment released from the end of the plasmid was then analyzed on a denaturing gel to assess processing of the 3′ terminus.

In these experiments, Artemis treatment consistently resulted in the generation of a prominent band that migrated just ahead of the 3′-PG 15-mer, at a position consistent with a 2-base 3′-hydroxyl overhang that would be formed by removal of the 3′-terminal nucleotide. In addition, a faint ladder of bands ≥14 bases in length was also generated, presumably reflecting nonspecific endonucleolytic cleavage. Nevertheless, generation of the putative 3′-hydroxyl 14-mer (but not the ladder) was completely dependent on AvaI treatment, indicating that it did not reflect cleavage near the site of radiolabel. Generation of the 3′-hydroxyl 14-mer was also completely dependent on Ku, DNA-PKcs and ATP, reflecting the known requirement for Artemis endonuclease activation by DNA-PKcs and ATP (3). No cleavage was detected when ATP was replaced with the nonhydrolyzable analogue adenosine 5′-O-(3-thiotriphosphate) (ATP-γS), consistent with a requirement for ATP hydrolysis (not shown). Additionally, there was no detectable Artemis-mediated formation of a 3′-hydroxyl 3-base overhang, suggesting that Artemis was not capable of cleaving the phosphodiester bond linking glycolate to the 3′ DNA end. These results indicate that activated Artemis selectively removes a single 3′-PG nucleotide from a 3-base 3′ overhang.

Under standard reaction conditions used with the oligomeric substrates, approximately 20% of the plasmid substrate with a 3′-PG-terminated 3-base overhang was specifically trimmed to the 2-base overhang product within 30 min, while there was no detectable trimming (<0.5%) of an analogous 3′-hydroxyl 3-base overhang substrate (Fig. 3). Longer incubations resulted in nearly complete removal of the terminal 3′-PG nucleotide, but there was significant loss of radiolabeled DNA overall, suggesting more extensive degradation of the substrate (Fig. 4). Consistent with results obtained using oligomeric substrates (Fig. 1C), addition of 35-bp duplex at a concentration (250-1000 nM) exceeding that of Ku, DNA-PKcs and Artemis suppressed the specific single-nucleotide trimming of the 3′-PG substrate, but stimulated nonspecific degradation (Fig. 4). Bands appearing above the PG-terminated 15-mer in these samples indicate cleavage >15 bases from the DNA end, and the labeled fragments must have been single-stranded as they were not cleaved by AvaI. Although the exact mechanism by which these fragments are produced remains to be determined, their generation was almost entirely Artemis-dependent (data not shown). Thus, one possibility is that, when DNA ends are in excess, ends not protected

by Ku and/or DNA-PKcs are subject to resection by the 5′→3′ exonuclease activity of Artemis, followed by endonucleolytic cleavage of the resulting 3′ overhang to release labeled single-strand fragments of various lengths.

There is evidence that DNA-PK activation requires synapsis of two DNA ends (21). In the present experiments, DNA ends are present at only ~2 nM and thus intramolecular synapsis of the plasmid ends is expected to be strongly favored. Due to the construction method (14), the unlabeled end of the plasmid bears a 10-base 5′ overhang. To determine whether the structure of this end influenced Artemis-mediated trimming, the plasmid was treated with AvrI, KpnI or StuI, all of which cut the plasmid near the unlabeled end leaving a 4-base 5′ overhang, a 4-base 3′ overhang, or a blunt end, respectively. Altering the unlabeled end of the plasmid had little effect on single-nucleotide trimming, suggesting that the overhang structure of the opposite end of the break was not critical to this process (data not shown).

In an attempt to reduce nonspecific cleavage of the plasmid substrate, the concentrations of Ku, DNA-PKcs, and Artemis were reduced from 65 nM, 50 nM, and 240 nM, respectively, to 13 nM, 35 nM and 90 nM. This change dramatically reduced degradation seen in the absence of Artemis, and also unexpectedly increased the efficiency of Artemis-mediated trimming, which was 50% complete in 30 min (Fig. 5A and 6A). To further define the requirements for Artemis-mediated PG processing, substrates with 3′-PG termini on a 2-base-recessed end, on a blunt end and on 3′ overhangs of 2, 3 and 4 bases, were constructed. Of these substrates, only the 3- and 4-base overhangs were efficiently processed (Fig. 5A). The 4-base overhang yielded approximately equal amounts of products corresponding to trimming of either 1 or 2 bases from the 3′ end. While substrates with shorter overhangs, blunt ends, or a recessed 3′ end all showed a small degree of 3′ processing, the cleavage was much less efficient as well as less specific, yielding multiple products of varied length. To verify the identity of the 14-mer band generated by Artemis from the 3′-PG substrate, the sample was subsequently treated with terminal transferase plus ddGTP, which produced the expected +1 nucleotide shift, demonstrating that the Artemis reaction product has a 3′-hydroxyl rather than a 3′-PG terminus (Fig. 5B). Moreover, both the putative 14-mer and the resulting 15-mer precisely comigrated with authentic markers of the predicted sequence.

Finally, substrates with 3-, 4-, 5- and 6-base overhangs, bearing both 3′-PG and 3′-hydroxyl termini, were constructed and subjected to treatment with Artemis/DNA-PK for 2-30 min (Fig. 6, left-hand panels show 3′-PG substrates). Under these conditions there was a trace of Artemis-dependent trimming of the 3′-hydroxyl 3-base overhang substrate, but it was still much less extensive as well as more heterogeneous than trimming of the 3′-PG (Fig. 6A). Quantitative phosphorimage analysis indicated that the initial rate of single-nucleotide removal was 10- to 20-fold greater for the PG-terminated than for the hydroxyl-terminated substrate (data not shown). For longer 3′-hydroxyl substrates (Fig. 6B-D, right panels), the predominant initial products indicated removal of 2 bases from the 3′ overhang, and none of these substrates showed removal of the terminal nucleotide alone. The substrate with a 3′-PG 4-base overhang again showed removal of either 1 or 2 nucleotides, but at the 5-min time point, single nucleotide removal was favored (~60% of the total cleavage, Fig. 6B). Similarly, for the 3′-PG 5-base overhang, single-nucleotide removal predominated at 5 min, while at later time points, removal of 2-3 nucleotides was more prevalent (Fig. 6C). Inasmuch as a 3′-hydroxyl 4-base overhang was efficiently trimmed to a 2-base overhang (Fig. 6C), the 3-base trimming of the 3′-PG 6-base overhang could occur in two steps: removal of the terminal 3′-PG nucleotide, followed by trimming of 2 additional nucleotides. Consistent with this possibility, the absolute amount of 5-base overhang clearly decreased after the first 5 min, while products with overhangs of 2-3 bases accumulated (Fig. 6D). A 13-base 3′-hydroxyl overhang also showed apparent two-step trimming, initially to 5 bases, and then to 3 bases (Fig. 7A).

Single-strand breaks formed by inhibitors of DNA topoisomerase I have the topoisomerase linked to the 3′ end of DNA via a 3′-phosphotyrosyl linkage, and these single-strand breaks can be converted to DSBs during DNA replication (22). To determine the susceptibility of such lesions to processing by Artemis, a substrate with a 3′-phosphotyrosyl on a 3-base overhang was prepared. Similar to the analogous 3′-PG substrate, this substrate was trimmed by 1 nucleotide when treated with Artemis, although somewhat less efficiently (Fig. 7B).

Thus, Artemis-mediated cleavage of 3′ overhangs appears to require at least 2 nucleotides between the double-strand/single-strand junction and the cleavage site, as well as either 2 nucleotides or a nucleotide plus a PG or phosphotyrosyl 3′ to the cleavage site (Fig. 7C). For short overhangs, a PG terminus has a strong effect on cleavage efficiency and specificity, but as the overhang length increases, the influence of the PG terminus rapidly diminishes.

Artemis-mediated PG processing in nuclear extracts—In human whole-cell extracts, most 3′-PG termini on partially complementary 3′ overhangs of DSBs are converted to 3′-hydroxyl termini by a combination of TDP1 and polynucleotide kinase/phosphatase (PNKP), and a substantial fraction of the breaks are rejoined, usually without loss of any terminal DNA nucleotides (20). However, in human nuclear extracts, most PG-terminated 3′ overhangs remain unprocessed even after several hours (10). The apparent failure of endogenous Artemis to process these lesions could be attributable to the limiting levels of Artemis in cell extracts. We therefore examined the possible effect of Artemis concentration on 3′-PG processing in this cell extract-based end joining assay. Linear plasmid substrates with a partially complementary (-ACG) 3-base 3′ overhang on each end, having either 3′-PG or 3′-hydroxyl termini, were incubated in HeLa nuclear extracts with or without exogenous Artemis. The plasmid was then cut with BstXI and Taq$^{\alpha}$I to release short fragments from both ends and thereby assess both end processing and DSB rejoining.

In unsupplemented extracts, there was substantial accurate end joining of the 3′-hydroxyl substrate, as indicated by the generation of a 42-base product (Fig. 8). Previous work showed that this repair is accomplished through annealing of the overhangs, fill-in of the 1-base gap by DNA polymerase λ, and ligation by XRCC4 / DNA ligase IV (15,20). With the 3′-PG substrate, there was a trace of accurate end joining, but most of the 3′-PG termini remained intact, with only ~21% being converted to 14-base 3′-hydroxyl termini. Addition of purified Artemis to these extracts resulted in apparent single-base trimming of the 3′-PG substrate to a 13 base product (10% of the total ends), as was seen with purified Artemis/DNA-PK alone. Moreover, addition of Artemis to reactions with the 3′-hydroxyl substrate reduced the abundance of the 42-base repair product, and other, shorter products of approximately 40, 37 and 29 bases were generated (arrows); a trace of the ~29-base product was also produced from the 3′-PG substrate. Although the exact mechanism of these repair events is uncertain, the results indicate that, in the context of DSB repair-competent cell extracts, Artemis can process protruding 3′-PG termini as well as promote error-prone end joining, apparently at the expense of accurate end joining.

Toxicity of 3′-phosphoglycolate-terminated DSBs in Artemis-deficient cells—The above data clearly show that Artemis can process 3′-PG-terminated DSBs. However, while hypersensitivity of Artemis-deficient mouse fibroblasts to bleomycin has been reported (23), a role for Artemis in processing of PG-terminated DSBs in intact human cells has not been established. To address this question, we assayed the toxicity of two drugs which induce different types of 3′-PG-terminated DSBs in vivo. Experiments measuring bromodeoxyuridine incorporation of ≥10,000 cells ~40 hours after treatment were used to calculate the proliferating fraction of cells. Bleomycin treatment gives rise to DSBs, nearly all of which have either blunt ends or single-base 5′ overhangs, with 5′-phosphate and 3′-PG termini at both ends of the break. Neocarzinostatin-induced DSBs have, at one end, a 5′-phosphate and a 3′-phosphate on a 2-base 3′ overhang; the opposite end has a 5′-aldehyde and either a 3′-phosphate or a 3′-PG on a 1-base 3′ overhang (17,18). We previously showed that fibroblasts from Artemis-deficient SCIDA patients exhibit significantly elevated sensitivity to X-irradiation but not to DSBs induced by etoposide (6). Here we find that hTERT immortalized SCIDA fibroblasts show hypersensitivity to the DSB-inducing agent bleomycin, albeit not as great as their sensitivity to X-rays. Interestingly, DSBs produced by neocarzinostatin, many of which bear overhanging 3′-PG termini, appear to be nearly as toxic to SCIDA cells as X-rays (Fig. 9A and Table 1). Similarly, treatment of SCIDA cells with X-rays, neocarzinostatin, and bleomycin, all which induce 3′-PG-terminated DSBs, results in much greater accumulation at G2/M in SCIDA cells than controls (Fig. 9B). Comparison of the relative toxicity of these three agents to controls reveals that toxicity is greatest with X-rays, intermediate with neocarzinostatin and lesser with bleomycin (Table 1). Multiple experiments revealed

qualitatively the same results with respect to the relative toxicity of these agents (not shown). These relative toxicities are consistent with the relative G2/M accumulation and the expected abundance of 3′ overhanging PG termini. Together, these data indicate that X-rays and radiomimetic drugs that induce DSBs with 3′-PG termini, result in lesions that require Artemis for resolution prior to continued cellular proliferation.

DISCUSSION

The data presented above show that, in the context of a variety of model DSB substrates, purified histidine-tagged Artemis efficiently cleaves long 3′ overhangs to a length of 4-5 nucleotides, in a reaction that is dependent on ATP and catalytically active DNA-PKcs. This specificity of cleavage, as well as the cofactor requirements, are in substantial agreement with results obtained using immobilized myc-tagged Artemis produced in human cells (3). The only apparent conflict with previous data is that, in our reactions with purified component proteins, Artemis activity is decisively enhanced in the presence of Ku heterodimer. Ku-dependent activation of DNA-PKcs is expected, inasmuch as Ku is normally required for efficient DNA-PK assembly and activation on DNA ends, except at very low ionic strength (24-26). The reported Ku independence for immobilized Artemis activity (3) may reflect the presence of specifically or nonspecifically coprecipitated Ku in the reactions; alternatively, immobilization of Artemis may influence the assembly and/or synapsis of DNA-PK/Artemis/DNA complexes.

Artemis-mediated trimming of long PG-terminated 3′-overhangs was qualitatively indistinguishable from that of the analogous 3′-hydroxyl overhangs (Fig. 2), but on very short overhangs, a PG terminus significantly altered cleavage specificity. For 3′-hydroxyl overhangs of 4-6 bases, the predominant initial site of Artemis-mediated cleavage was 2 bases from the 3′-terminus, but a 3′-PG terminus promoted removal of a single terminal nucleotide, an event rarely seen with unmodified overhangs (Fig. 6). This difference in specificity was most dramatic for a 3-base 3′-PG overhang, from which Artemis efficiently and specifically removed the single 3′-terminal nucleotide, while the leaving the analogous 3′-hydroxyl substrate largely intact (Fig. 3). However, the efficiency of single-nucleotide trimming of PG-terminated substrates decreased sharply with increasing overhang length, such that for a 6-base overhang only a trace of single-nucleotide trimming was detected (Fig. 6).

Thus, the site of Artemis-mediated cleavage of 3′-overhangs appears to be dependent on three criteria: 1) a requirement for either 2 nucleotides or a nucleotide plus a 3′-PG 3′ to the cleavage site, 2) a requirement for at least 2 unpaired nucleotides 5′ to the cleavage site, and 3) a preference for cleavage 4-5 bases from the single-strand/double-strand transition (Fig. 7C). It is likely that for long overhangs positioning of DNA-PK at the single-strand/double-strand transition positions the Artemis active site for cleavage 4-5 bases from the transition. There appears to be some flexibility in this positioning, however, and on shorter overhangs the positioning is preempted by the more stringent requirement for 2 nucleotides (or nucleotide-plus-PG) 3′ to the cleavage site; presumably, the endonucleolytic activity of Artemis requires that it form molecular contacts with these 2 nucleotides, the last of which can be substituted by a PG. Unmodified overhangs shorter than 4 bases, and PG-terminated overhangs shorter than 3 bases, are much less efficiently processed, likely due to the fact that the requirements for 2 bases 3′ and 2 unpaired bases 5′ of the cleavage site cannot be simultaneously satisfied.

Despite strong evidence for involvement of Artemis in nonhomologous DNA end joining, we and others have shown that the majority of radiation-induced DSBs can be rapidly rejoined in the absence of Artemis (4-6). However, at both 6 and 24 hr after irradiation, Artemis-deficient cells exhibit approximately twofold more residual γ-H2AX foci/nucleus than wild type controls, suggesting that a subpopulation of DSBs in these cells is resistant to repair in the absence of Artemis (6). Psuedo-epistasis studies using a combination of kinase inhibitors and genetic defects, suggest that repair of these breaks requires not only Artemis and DNA-PK, but also the ataxia telangiectasia-mutated (ATM) kinase as well as proteins typically found in DSB repair foci such as 53BP1 and the Mre11/Rad50/NBS1 (MRN) complex (5). It is presently unclear what types of DSBs strictly require Artemis, but the finding that a greater proportion of α-particle-induced DSBs (~20%) than of X-ray-induced DSBs (~10%) require Artemis for repair suggests that chemical complexity of the breaks may be a factor (5).

However, unlike radiation, the radiomimetic agents neocarzinostatin and bleomycin are not thought to induce any locally multiply damaged sites, such as DSBs accompanied by nearby base damage (17, 18). Yet, SCIDA cells show hypersensitivity to neocarzinostatin and bleomycin as well as to X-rays, suggesting that 3′-PG and/or 5′-aldehyde DSB termini alone at a DSB may represent relevant in vivo substrates for Artemis.

Biochemical studies presented here suggest that PG-terminated DSBs induced by bleomycin and neocarzinostatin (which are either blunt or with single-base 5′ or 3′ overhangs) can indeed be processed by Artemis, albeit much less efficiently than breaks with longer 3′ overhangs (Fig. 5). Radiation presumably induces DSBs with a random stagger, and therefore many radiation-induced breaks will bear PG-terminated 3′ overhangs of ≥3 bases, lesions that are processed very efficiently by Artemis. Although in no case is the overhang fully preserved, on short overhangs removal of only a single nucleotide is favored, thus potentially minimizing the frequency and size of deletions resulting from the repair. The only other enzyme known to be capable of processing 3′-PG termini on 3′ overhangs is TDP1 (9). However, the finding that TDP1-deficient cells are at most only marginally sensitive to X-rays (10) (which induce a large proportion of PG-terminated DSBs (7)), suggests that the end joining pathway may preferentially utilize Artemis for processing, despite the fact that it would be more likely than TDP1 to produce small deletions at the DSB site. At the very least, Artemis can provide a backup pathway for breaks that elude processing by TDP1.

Alternatively, Artemis may not be strictly required for processing 3′-PG DSBs, but instead may function in the resolution of derivative structures that can arise from them. In principle, a 3′-PG terminus will block gap-filling and ligation, but allow 5′→3′ resection by the MRN complex or other nucleases. Artemis, in the presence of DNA-PK, is capable of trimming any resulting blocked 3′ overhangs while they are still very short, at which point gap-filling and ligation can proceed. However, blocked 3′ termini not resolved at this point may result in more extensive 5′ resection. Such resection in the context of an inverted repeat may lead to the formation of hairpin-like termini via annealing of the 3′ overhangs. This sequence of events would convert a fraction of 3′-blocked DSBs that were initially repairable by DNA-PK, TDP1, PNKP, polymerase λ, and ligase IV (8), to structures that strictly require Artemis for resolution. Thus, a failure to resolve 3′-PG structures at an early stage in the repair pathway could lead to an increased incidence of repair-resistant derivative structures, either the long 3′ overhangs themselves or resulting hairpins. The observed accumulation of Artemis-deficient cells in G2/M is consistent with the evolution of unresolvable derivative DNA structures in Artemis-deficient cells. Moreover, in contrast to X-rays, DSBs induced by the topoisomerase II inhibitor etoposide, are not selectively toxic to SCIDA cells (6). While etoposide-induced DSBs are terminally blocked, these DSBs bear protein-linked 5′ termini and would not be subject to 5′ resection.

In summary, our results demonstrate that Artemis has the capability to carry out an essential step in repair of radiation-induced DNA damage—elimination of the 3′-PG blocking lesions commonly found at DSB termini. Although Artemis lacks the specificity to remove only the 3′-PG, it can nevertheless resolve this type of lesion by excising the terminal nucleotide along with the contiguous 3′-PG moiety. This activity is only expressed in the context of the core nonhomologous end joining proteins Ku and (catalytically active) DNA-PKcs. Moreover, like X-rays, agents that induce well-characterized PG-terminated DSBs show elevated toxicity and cause G2/M accumulation of Artemis-deficient human cells. Both these findings suggest that resolution of PG-terminated DSBs is relevant to Artemis function in DNA repair, and may provide at least a partial explanation for the radiosensitivity of Artemis-deficient cells.

Acknowledgments— We thank Hector Nolla at the UC Berkeley flow cytometer facility for his assistance and Drs. Altaf Sarker and David J. Chen for helpful discussions.

[1]The abbreviations used are: DNA-PK, DNA-dependent protein kinase; DNA-PKcs, DNA-PK catalytic subunit; DSB, double-strand break PG, phosphoglycolate; PNKP, polynucleotide kinase/phosphatase; SCID, severe combined immune deficiency; TDP1, tyrosyl-DNA phosphodiesterase.

REFERENCES

1. Moshous, D., Callebaut, I., de Chasseval, R., Corneo, B., Cavazzana-Calvo, M., Le Deist, F., Tezcan, I., Sanal, O., Bertrand, Y., Philippe, N., Fischer, A., and de Villartay, J.P. (2001) *Cell* **105**, 177-186

2. Li, L., Moshous, D., Zhou, Y., Wang, J., Xie, G., Salido, E., Hu, D., de Villartay, J.P., and Cowan, M.J. (2002) *J. Immunol.* **168**, 6323-6329

3. Ma, Y., Pannicke, U., Schwarz, K., and Lieber, M.R. (2002) *Cell* **108**, 781-794

4. Nicolas, N., Finnie, N.J., Cavazzana-Calvo, M., Papadopoulo, D., Le Deist, F., Fischer, A., Jackson, S.P., and de Villartay, J.P. (1996) *Eur. J. Immunol.* **26**, 1118-1122

5. Riballo, E., Kuhne, M., Rief, N., Doherty, A., Smith, G.C., Recio, M.J., Reis, C., Dahm, K., Fricke, A., Krempler, A., Parker, A.R., Jackson, S.P., Gennery, A., Jeggo, P.A., and Löbrich, M. (2004) *Mol. Cell* **16**, 715-724

6. Wang, J., Pluth, J.M., Cooper, P.K., Cowan, M.J., Chen, D.J., and Yannone, S.M. (2005) *DNA Repair* **4**, 556-570

7. Henner, W.D., Rodriguez, L.O., Hecht, S.M., and Haseltine, W.A. (1983) *J. Biol. Chem.* **258**, 711-713

8. Valerie, K. and Povirk, L.F. (2003) *Oncogene* **22**, 5792-5812

9. Inamdar, K.V., Pouliot, J.J., Zhou, T., Lees-Miller, S.P., Rasouli-Nia, A., and Povirk, L.F. (2002) *J. Biol. Chem.* **276**, 24323-24330

10. Zhou, T., Lee, J.W., Tatavarthi, H., Lupski, J.R., Valerie, K., and Povirk, L.F. (2005) *Nucleic Acids Res.* **33**, 289-297

11. Yannone, S.M., Roy, S., Chan, D.W., Murphy, M.B., Huang, S., Campisi, J., and Chen, D.J. (2001) *J. Biol. Chem.* **276**, 38242-38248

12. Hsu, H.-L., Yannone, S.M., and Chen, D.J. (2001) *DNA Repair* **1**, 225-235

13. Chen, S., Hannis, J.C., Flora, J.W., Muddiman, D.C., Charles, K., Yu, Y., and Povirk, L.F. (2001) *Anal. Biochem.* **289**, 274-280

14. Bennett, R.A.O., Gu, X.-Y., and Povirk, L.F. (1996) *Intl. J. Radiat. Biol.* **70**, 623-636

15. Lee, J.W., Blanco, L., Zhou, T., Bebenek, K., Garcia-Diaz, M., Kunkel, T.A., Wang, Z., and Povirk, L.F. (2004) *J. Biol. Chem.* **279**, 805-811

16. Huang, J. and Dynan, W.S. (2002) *Nucleic Acids Res.* **30**, 667-674

17. Dedon, P.C. and Goldberg, I.H. (1992) *Chem. Res. Toxicol.* **5**, 311-332

18. Povirk, L.F. (1996) *Mutat. Res.* **355**, 71-89

19. Bertoncini, C.R. and Meneghini, R. (1995) *Nucleic Acids Res.* **23**, 2995-3002

20. Chen, S., Inamdar, K.V., Pfeiffer, P., Feldmann, E., Hannah, M.F., Yu, Y., Lee, J.W., Zhou, T., Lees-Miller, S.P., and Povirk, L.F. (2001) *J. Biol. Chem.* **276**, 24323-24330

21. DeFazio, L.G., Stansel, R.M., Griffith, J.D., and Chu, G. (2002) *EMBO J.* **21**, 3192-3200

22. D′Arpa, P. and Liu, L.F. (1989) *Biochim. Biophys. Acta* **989**, 163-177

23. Rooney, S., Alt, F.W., Lombard, D., Whitlow, S., Eckersdorff, M., Fleming, J., Fugmann, S., Ferguson, D.O., Schatz, D.G., and Sekiguchi, J. (2003) *J. Exp. Med.* **197**, 553-565

24. Gottlieb, T.M. and Jackson, S.P. (1993) *Cell* **72**, 131-142

25. West, R.B., Yaneva, M., and Lieber, M.R. (1998) *Mol. Cell Biol.* **18**, 5908-5920

26. Hammarsten, O. and Chu, G. (1998) *Proc. Natl. Acad. Sci. U. S. A.* **95**, 525-530

FOOTNOTES

*This work was supported by grant CA40615 from the National Cancer Institute, US DHHS and the Office of Science, US Department of Energy, under Contract No. DE-AC03-76SF00098 through the Low Dose Radiation Research Program and NIH grants AI28339 and HL58842.

FIGURE LEGENDS

Fig. 1. Trimming of 3′-hydroxyl-terminated 3′ overhangs in partial duplexes by Artemis nuclease. (A) Cleavage of a 13-base (36/23), 15-base (36/21) or 17-base (36/19) overhang by Artemis (240 nM) in the presence of Ku (65 nM), DNA-PKcs (50 nM), and an excess of blunt-ended double-stranded (DS) 35-mer (0.5 μM). Samples were incubated for 15 or 60 min and analyzed on a sequencing gel along side a Maxam-Gilbert A+G chemical cleavage marker. (B) Effect of Ku and the double-stranded 35-mer on cleavage. Incubation time was 30 min and other conditions were the same as above. (C) Concentration-dependent inhibition of Artemis-mediated trimming of the 13-base overhang, by the double-stranded 35-mer (4, 16, 60, 250 and 1000 nM).

Fig. 2. Artemis efficiently shortens long 3′ overhangs bearing 3′-hydroxyl or 3′-PG termini. Oligomeric substrates with a 17-base (36/19), 15-base (36/21), 13-base (36/23) or 9-base (36/27p) 3′ overhang, and bearing a 3′-hydroxyl terminus (A) or a 3′-PG terminus (B) were treated with Artemis plus DNA-PK for 30 min. The 27-mer was 5′-phosphorylated but the other complementary strands were not. Protein concentrations are the same as in Fig. 1. Note that the substrates are internally labeled 14 bases from the 3′ end. Thus, the Artemis cleavage products, which bear both 5′- and 3′-hydroxyls, run a full nucleotide position more slowly than Maxam-Gilbert markers of the same length, which bear 5′- and 3′-phosphates; for example, the 31-base cleavage product from the 36/27p duplex comigrates with the 32-base marker generated by chemical cleavage of the G at position 33 in the sequence (..CGCGACG).

Fig. 3. Artemis trims a single nucleotide from a PG-terminated 3-base 3′ overhang. An internally labeled (*) plasmid substrate with a PG- (●) or hydroxyl-terminated 3′ overhang was treated with Artemis (240 nM) in the presence of Ku (65 nM) and DNA-PKcs (50 nM) for 30 min, then cut with AvaI and the products analyzed on a sequencing gel. Various reaction components were omitted as indicated. Numbers to the right of the gel indicate overhang length. Inset at bottom shows material that remained in the loading well, presumably plasmid that was not cut by AvaI.

Fig. 4. Time course of single-nucleotide trimming by Artemis and effect of double-stranded 35-mer. The plasmid substrate with a 3-base PG-terminated 3′ overhang (shown in Fig. 3) was treated with Artemis for various times in the presence of Ku and DNA-PKcs, then cut with AvaI. Numbers to the right of the gel indicate overhang length. Concentrations of the 35-mer were 4, 16, 60, 250 and 1000 nM. Protein concentrations were as in Fig. 3.

Fig. 5. Artemis activity on a plasmid bearing a 3′-PG (●) on a 2-, 3- or 4-base 3′ overhang, a blunt end, or a 2-base-recessed 3′ end. (A) Samples were treated for 30 min with 90 nM Artemis, 35 nM DNA-PKcs and 13 nM Ku, and then treated with AvaI. Arrows show the major cleavage sites. (B) Terminal transferase-mediated extension the 3′-hydroxyl terminus generated by Artemis-mediated trimming of a 3′-PG-terminated 3-base overhang. Following treatment with Artemis and AvaI as above, samples were treated with terminal transferase (TdT) plus ddGTP. Lanes marked “M” contain 5′-end-labeled 14- or 15-base fragments of the expected sequence (TCGAGGAACGCGAC and TCGAGGAACGCGACG, respectively). Numbers to the right indicate overhang length.

Fig. 6. Artemis activity on a plasmid bearing either a 3′-PG (·) or a 3′-hydroxyl on a 3-, 4- 5- or 6-base 3′ overhang. Samples were treated for the indicated times with 90 nM Artemis, 35 nM DNA-PKcs and 13 nM Ku, and then treated with Taq$^{\alpha}$I. Arrows show the major initial cleavage sites. Numbers to right indicate overhang length.

Fig. 7. Artemis activity on a plasmid bearing either a 3′-hydroxyl-terminated 13-base

3′ overhang (A) or a 3′-phosphotyrosine (pTyr) -terminated 3-base 3′ overhang (B). Conditions are the same as in Fig. 6. Arrows show the major initial cleavage sites. Numbers to right indicate overhang length. A model summarizing the requirements for trimming of 3′ overhangs by Artemis is presented (C).

Fig. 8. Effect of exogenous Artemis on DSB end processing and end joining in HeLa nuclear extracts. The internally labeled (*) substrate shown, with either 3′-PG or 3′-hydroxyl termini, was incubated for 6 hr in HeLa nuclear extracts supplemented with XRCC4 / DNA ligase IV (25 nM). Exogenous Artemis (75 nM) was added to some samples as indicated. Samples were treated with BstXI and Taq$^{\alpha}$I and analyzed on a denaturing sequencing gel. BstXI cuts 27 bases from the 5′ terminus. The major repair product, comigrating with a synthetic 42-base marker of the expected sequence ("M"), corresponds to annealing of the terminal CG in the overhang, fill-in of the 1-base gap and ligation; the 24-base product corresponds to similar joining of two plasmid molecules head-to-head. Arrows show shorter repair products, the formation of which was promoted by Artemis. Numbers show actual length of labeled fragments, not the overhang length.

Fig. 9. Cellular proliferation assays showing response of wild type (AK) and SCIDA (04 and 05) cells to various genotoxic agents. (A) The fraction of proliferating cells (% BrdU positive) was determined approximately 40 hours after the indicated genotoxic treatments of either X-rays or one hour exposure to either bleomycin or neocarzinostatin. (B) Cell cycle distribution of wild type (AK) and SCIDA (04 and 05) fibroblasts approximately 40 hours after mock treatment (control), 5 Gy X-rays, one hour exposure to 7.5 nM neocarzinostatin or 10 μg/ml bleomycin (≥ 10,000 events/point were scored).

	AK (wt)	04 (SCIDA)	05 (SCIDA)	Ratio[a] (SCIDA/wt)
X-Rays (5 Gy)	62.5	26.1	25.3	0.411
Neocarzinostatin (10 nM)	63.0	30.7	35.1	0.522
Bleomycin (2.5 μg/ml)	63.5	53.2	48.0	0.801

Table 1. Quantitative measurements of the proliferating fraction of cells (%) after the indicated treatments. [a.]The ratios are calculated from the average of the SCIDA cell values divided by the wild type values from the same treatments.

Figure 1

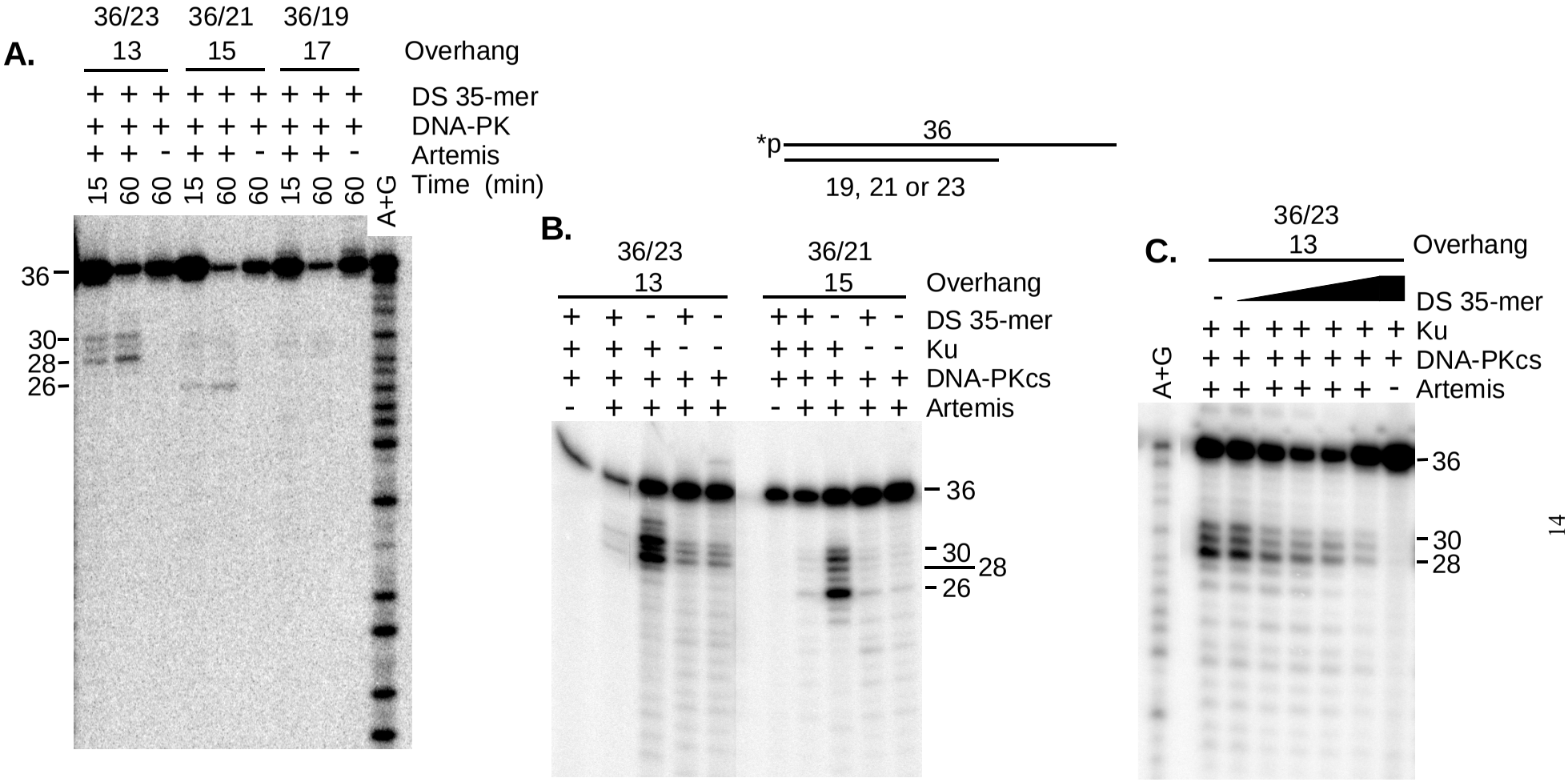
A.
36/23
13
36/21
15
36/19
17
Overhang
DS 35-mer
DNA-PK
Artemis
Time (min)
15 60 60 15 60 60 15 60 60 A+G
36
30
28
26
*p
36
19, 21 or 23
B.
36/23
13
36/21
15
Overhang
DS 35-mer
Ku
DNA-PKcs
Artemis
36
30
28
26
C.
36/23
13
Overhang
DS 35-mer
Ku
DNA-PKcs
Artemis
A+G
36
30
28

Figure 2

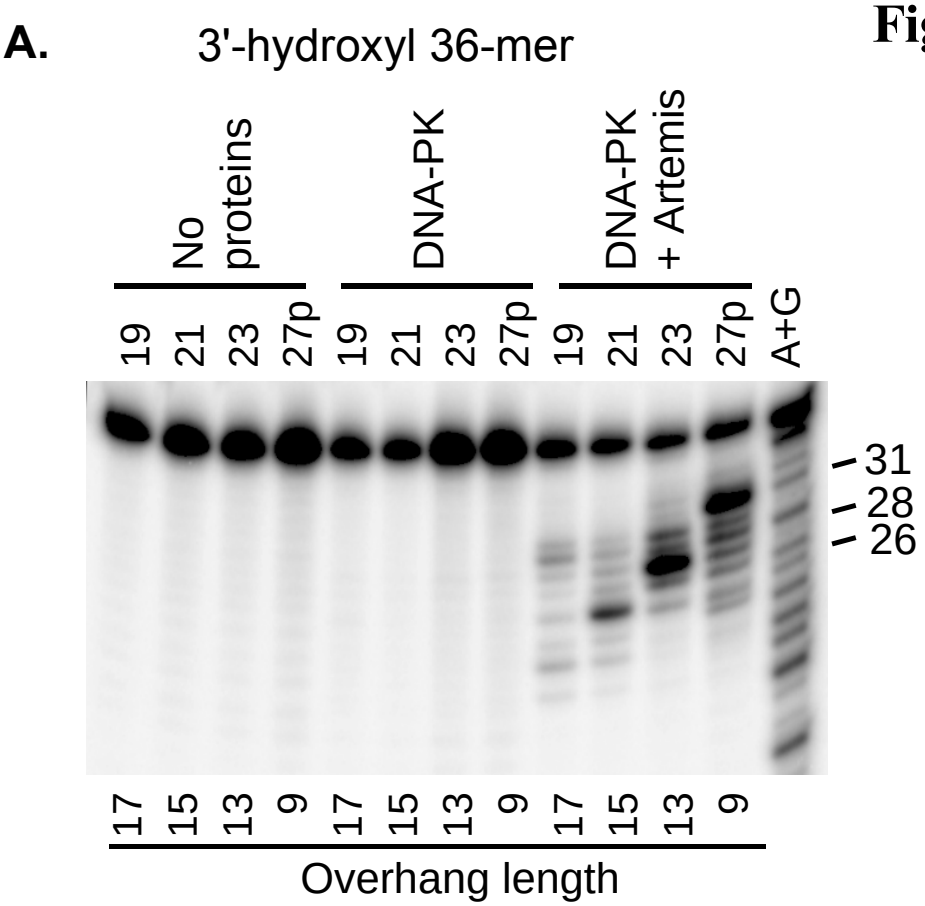
A.
3'-hydroxyl 36-mer
No proteins
DNA-PK
DNA-PK + Artemis
19 21 23 27p 19 21 23 27p 19 21 23 27p A+G
31
28
26
17 15 13 9 17 15 13 9 17 15 13 9
Overhang length

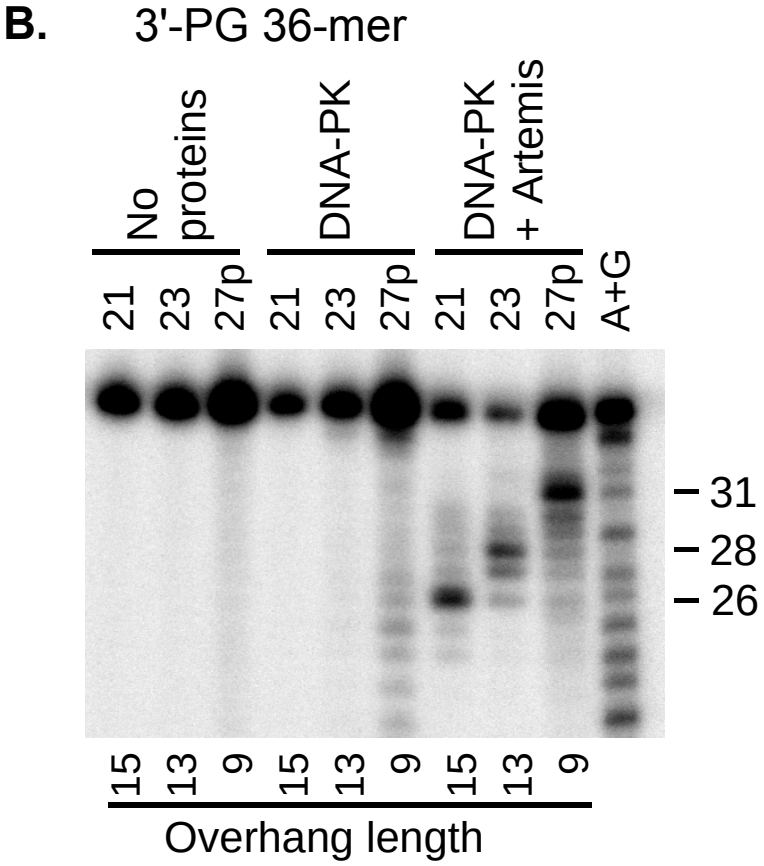
B.
3'-PG 36-mer
No proteins
DNA-PK
DNA-PK + Artemis
21 23 27p 21 23 27p 21 23 27p A+G
31
28
26
15 13 9 15 13 9 15 13 9
Overhang length

Figure 3

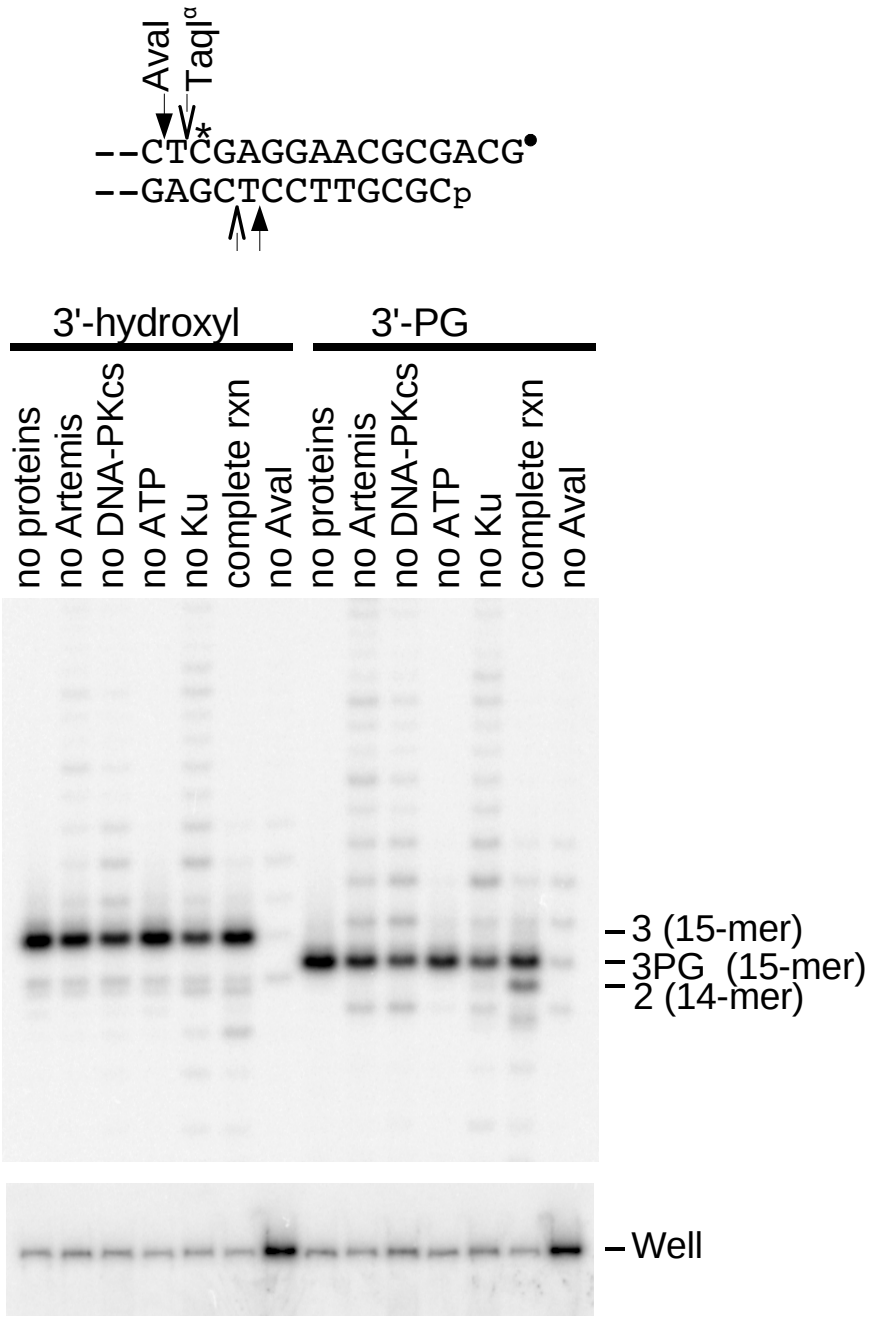
AvaI
TaqI$^{\alpha}$
--CTCGAGGAACGCGACG•
--GAGCTCCTTGCGCp
3'-hydroxyl
3'-PG
no proteins
no Artemis
no DNA-PKcs
no ATP
no Ku
complete rxn
no AvaI
3 (15-mer)
3PG (15-mer)
2 (14-mer)
Well

Figure 4

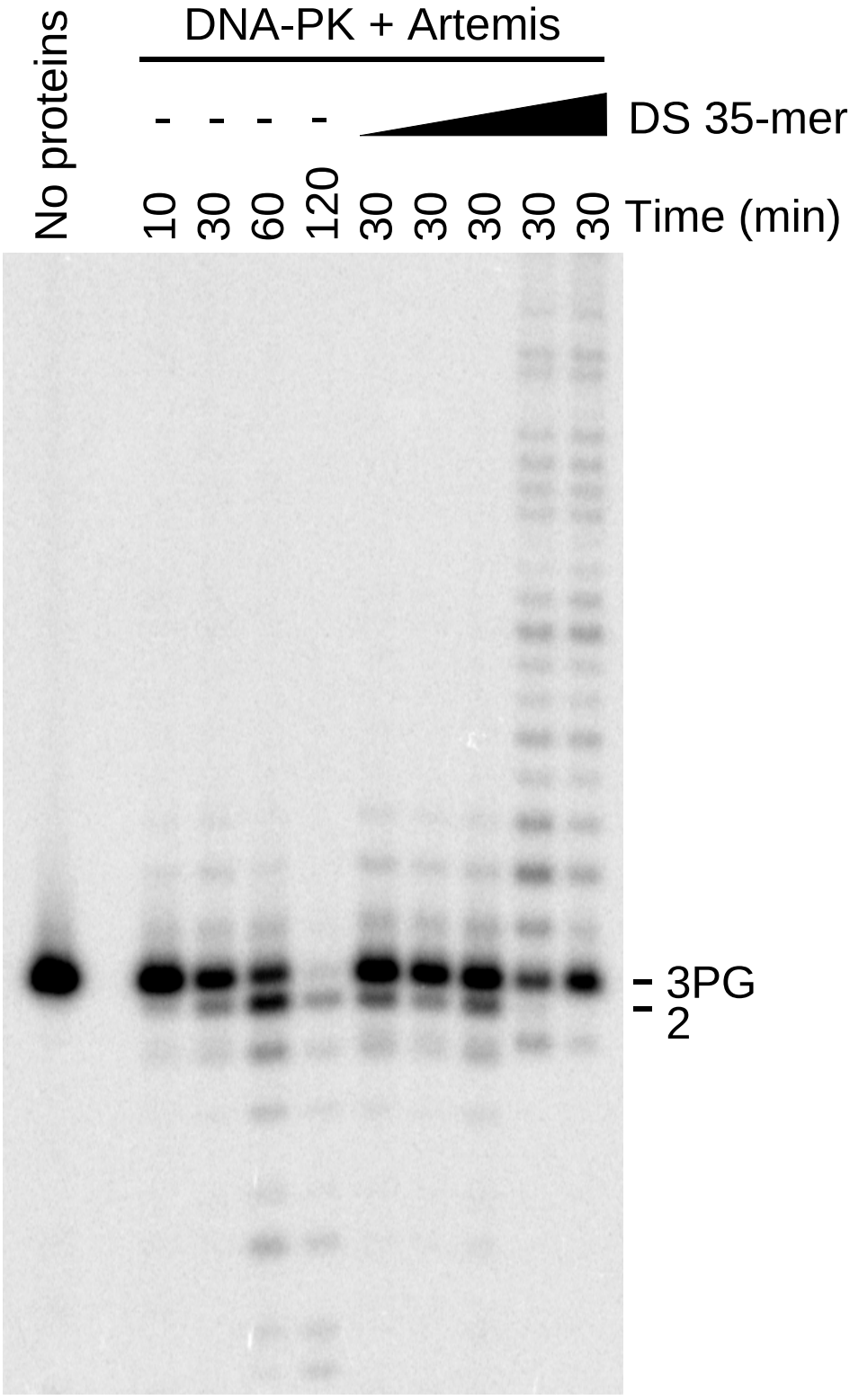
No proteins
DNA-PK + Artemis
- - - -
DS 35-mer
10 30 60 120 30 30 30 30 30
Time (min)
3PG
2

Figure 5

A.

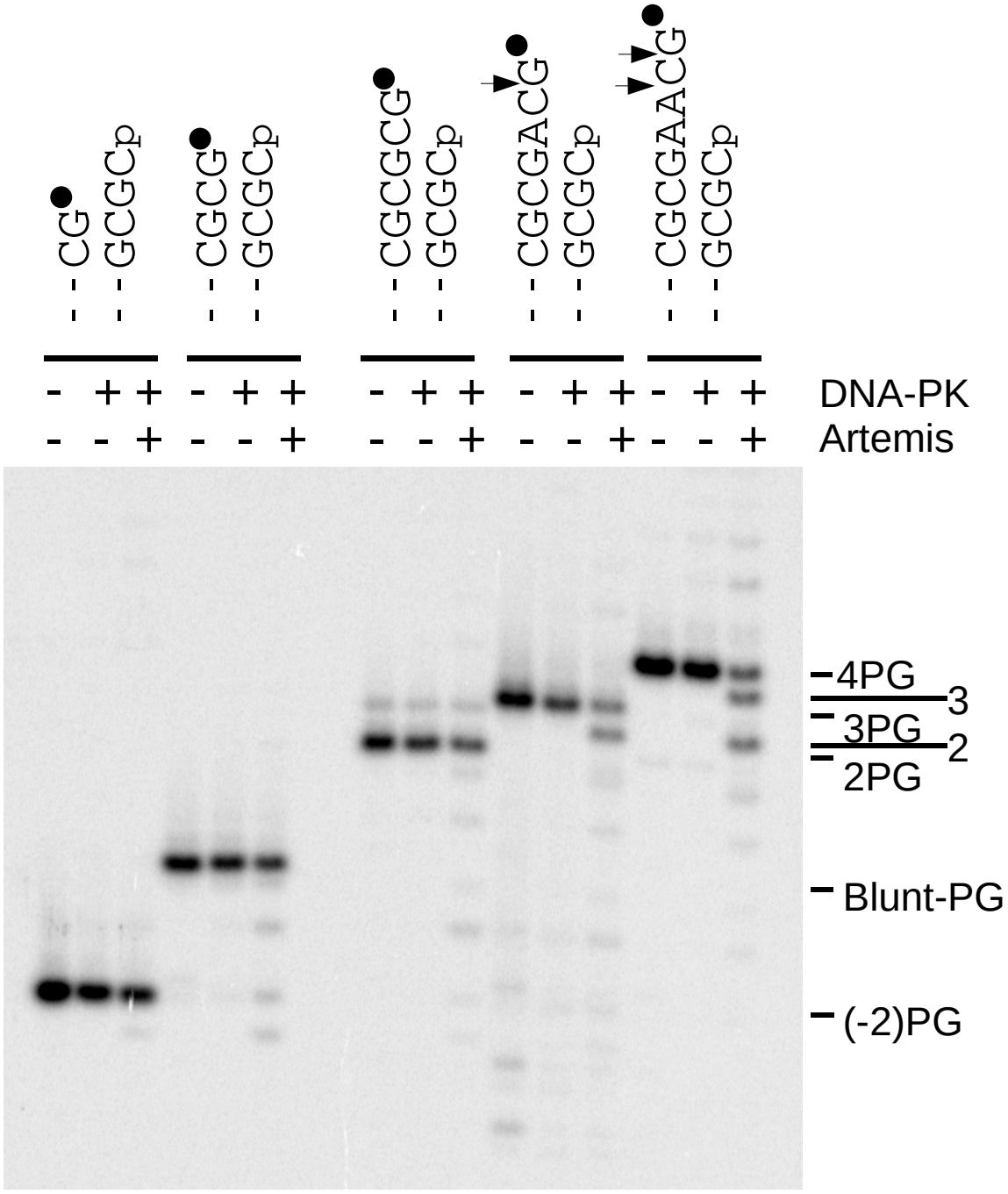
CG
GCGCp
CGCG
GCGCp
CGCGCG
GCGCp
CGCGACG
GCGCp
CGCGAACG
GCGCp
DNA-PK
Artemis
4PG
3
3PG
2
2PG
Blunt-PG
(-2)PG

B.

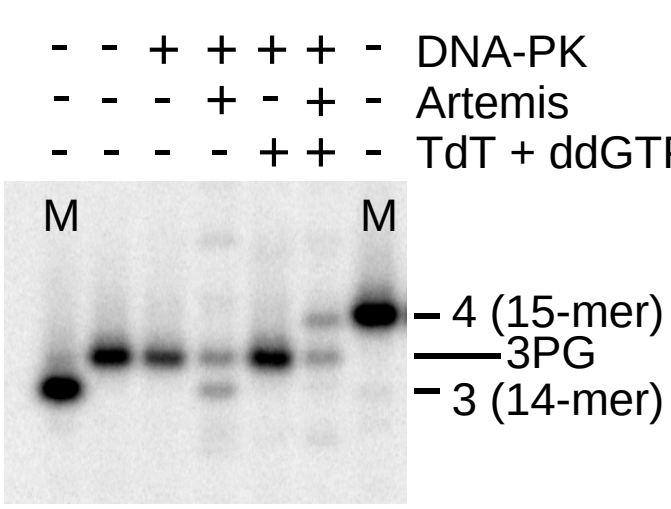
DNA-PK
Artemis
TdT + ddGTP
M
M
4 (15-mer)
3PG
3 (14-mer)

Figure 6

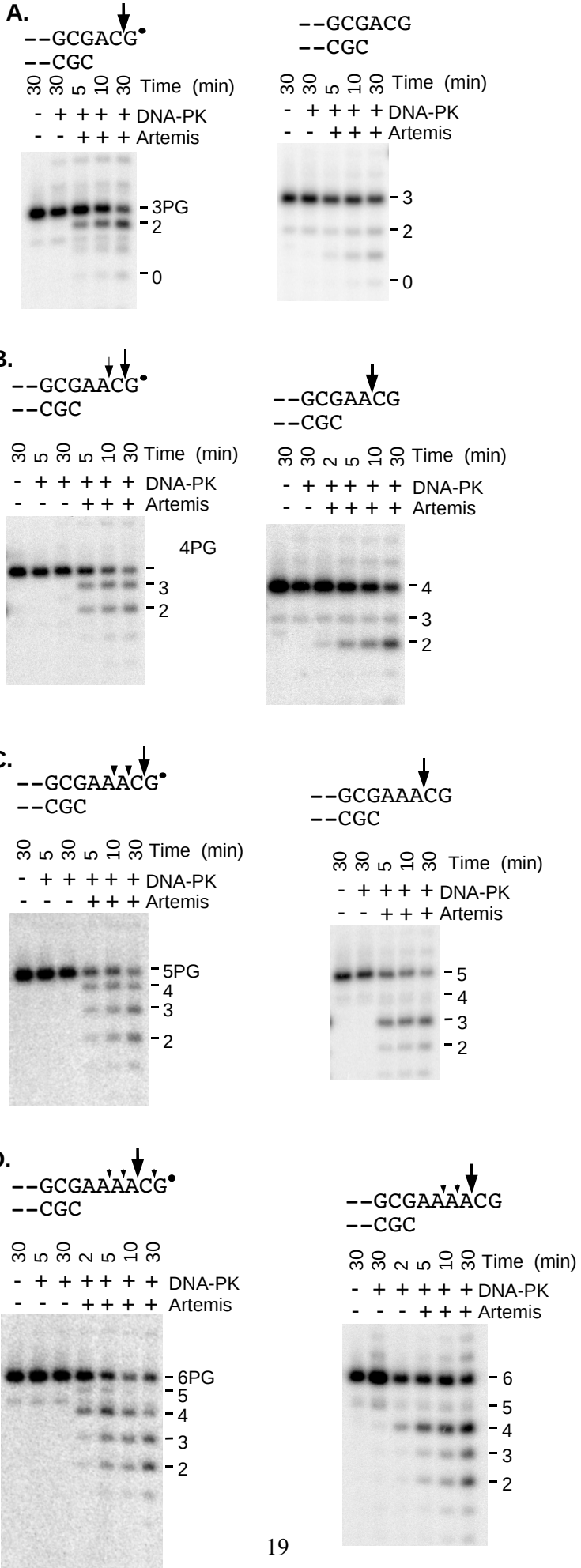
A.
--GCGACG•
--CGC
30 30 5 10 30 Time (min)
- + + + + DNA-PK
- - + + + Artemis
3PG
2
0
--GCGACG
--CGC
30 30 5 10 30 Time (min)
- + + + + DNA-PK
- - + + + Artemis
3
2
0
B.
--GCGAACG•
--CGC
30 5 30 5 10 30 Time (min)
- + + + + + DNA-PK
- - - + + + Artemis
4PG
3
2
--GCGAACG
--CGC
30 30 2 5 10 30 Time (min)
- + + + + + DNA-PK
- - + + + + Artemis
4
3
2
C.
--GCGAAACG•
--CGC
30 5 30 5 10 30 Time (min)
- + + + + + DNA-PK
- - - + + + Artemis
5PG
4
3
2
--GCGAAACG
--CGC
30 30 5 10 30 Time (min)
- + + + + DNA-PK
- - + + + Artemis
5
4
3
2
D.
--GCGAAAACG•
--CGC
30 5 30 2 5 10 30
- + + + + + + DNA-PK
- - - + + + + Artemis
6PG
5
4
3
2
--GCGAAAACG
--CGC
30 30 2 5 10 30 Time (min)
- + + + + + DNA-PK
- - - + + + Artemis
6
5
4
3
2

Figure 7

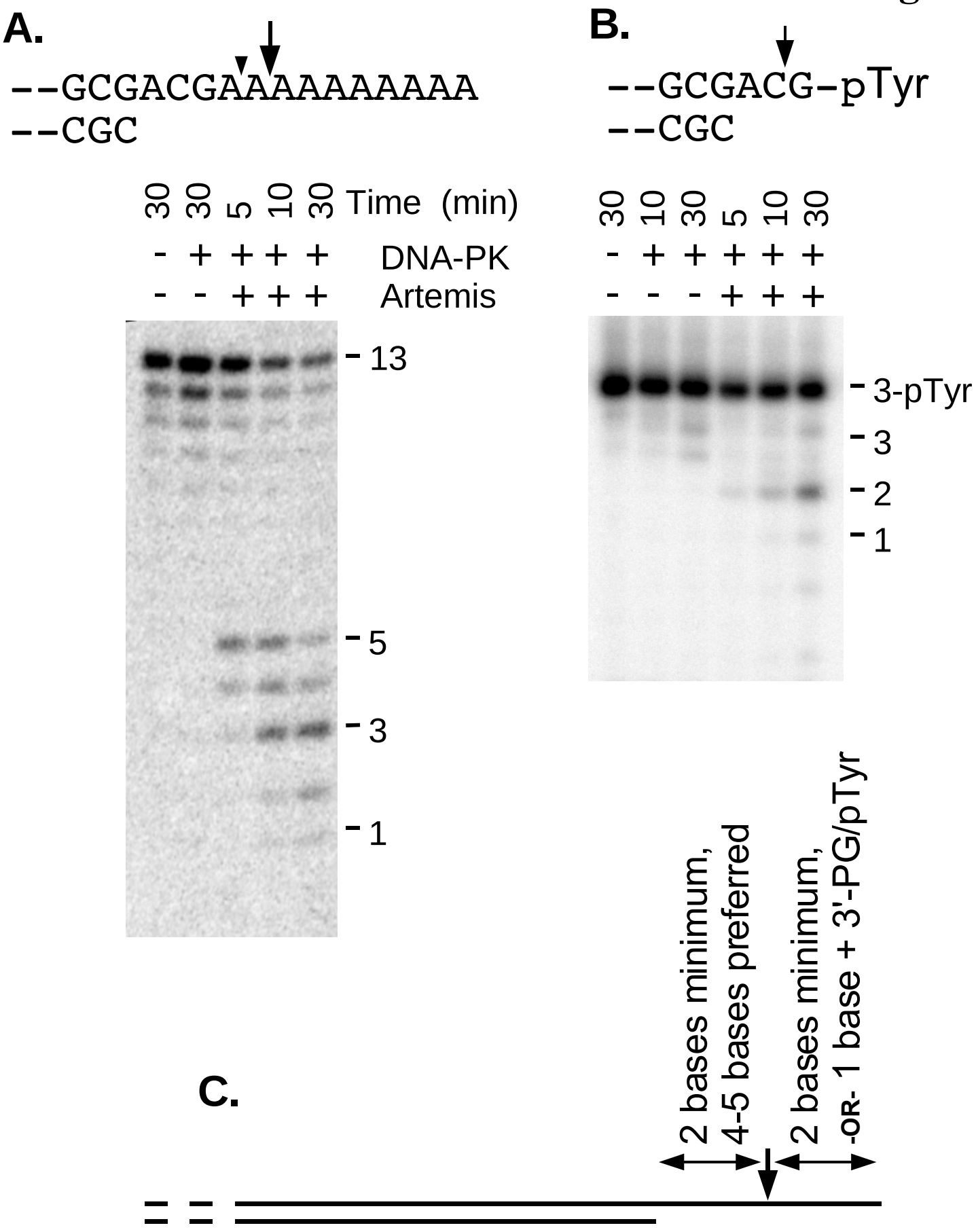
A.
--GCGACGAAAAAAAAAA
--CGC
30 30 5 10 30 Time (min)
- + + + + DNA-PK
- - + + + Artemis
13
5
3
1
B.
--GCGACG-pTyr
--CGC
30 10 30 5 10 30
- + + + + +
- - - + + +
3-pTyr
3
2
1
C.
2 bases minimum,
4-5 bases preferred
2 bases minimum,
-OR- 1 base + 3'-PG/pTyr

Figure 8

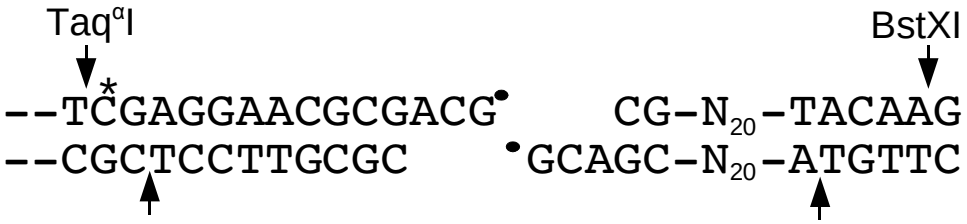
Taq^αI
BstXI
--TCGAGGAACGCGACG
CG-N20-TACAAG
--CGCTCCTTGCGC
GCAGC-N20-ATGTTC

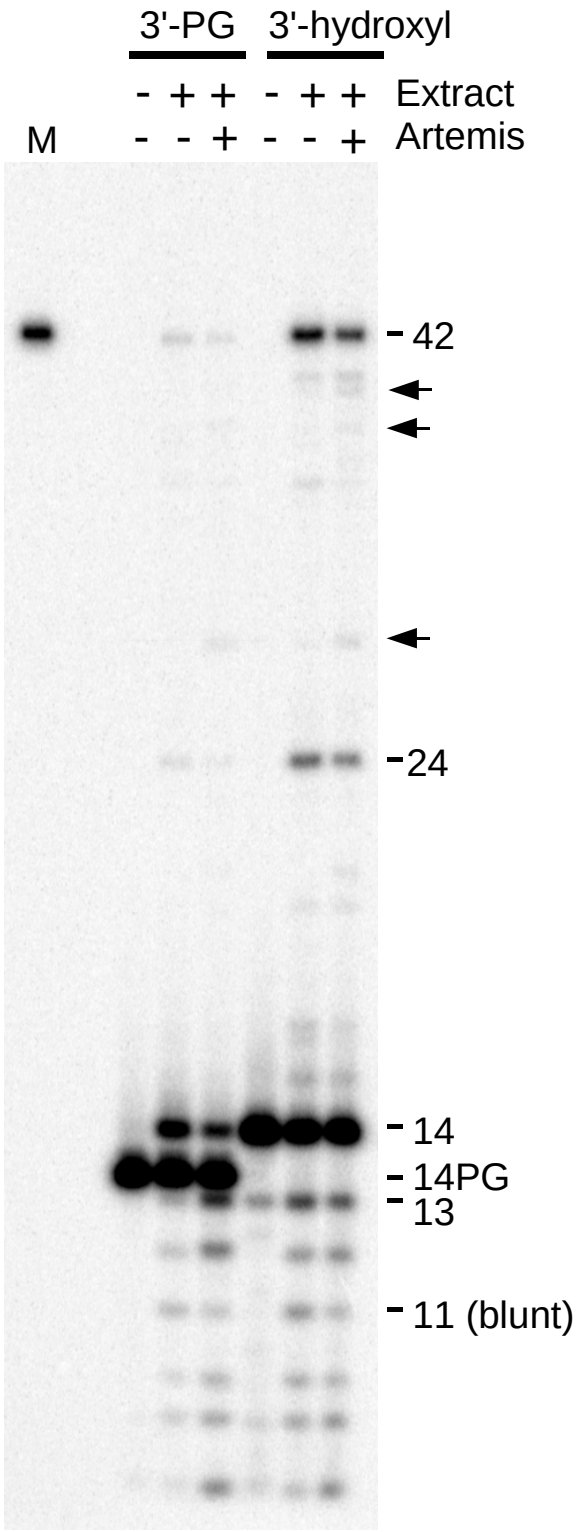
3'-PG
3'-hydroxyl
- + + - + + Extract
M - - + - - + Artemis
42
24
14
14PG
13
11 (blunt)

Figure 9.

A

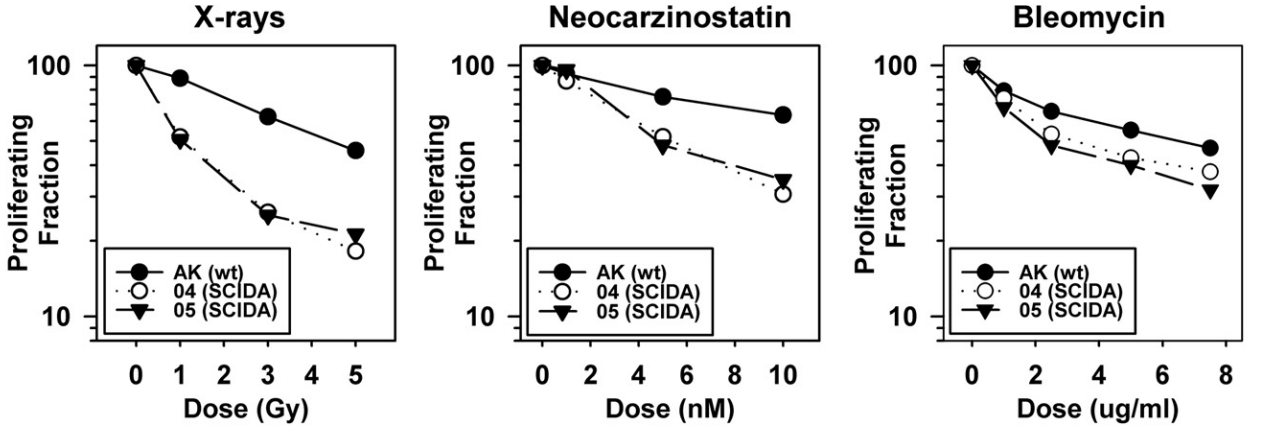
X-rays
Neocarzinostatin
Bleomycin
Proliferating Fraction
100
10
AK (wt)
04 (SCIDA)
05 (SCIDA)
0 1 2 3 4 5
Dose (Gy)
0 2 4 6 8 10
Dose (nM)
0 2 4 6 8
Dose (ug/ml)

B

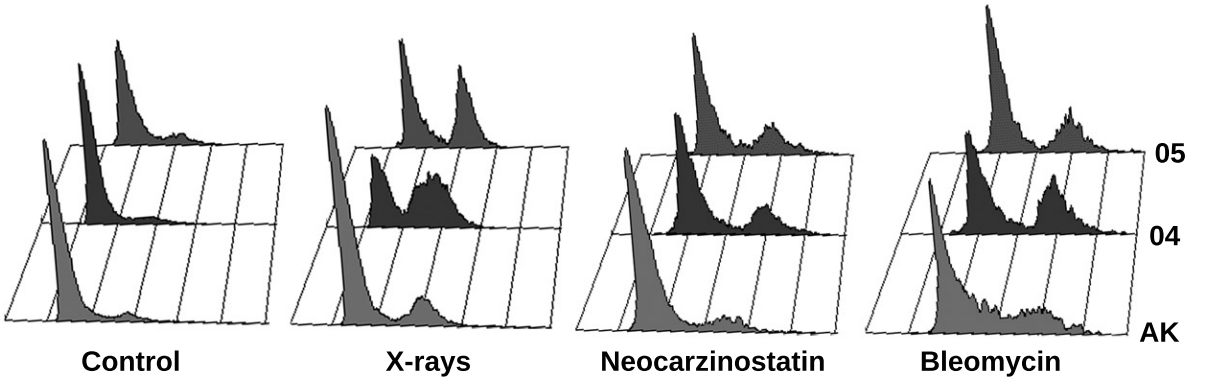
05
04
AK
Control
X-rays
Neocarzinostatin
Bleomycin